11. Cason, *J. Org. Synth. Collective Volume 3*, **1995**, p 3.
12. Yanagisawa, H.; Ando, A.; Shiozaki, M.; Hiraoka, T. *Tetrahedron Lett.* **1983**, *24*, 1037.
13. Gupta, D.; Soman, R.; Dev, S. *Tetrahedron* **1982**, *38*, 3013.

Molecular Dynamics Simulation of Liquid Alkanes. II. Dynamic Properties of Normal Alkanes : *n*- Butane to *n*- Heptadecane

Song Hi Lee*, Hong Lee, and Hyungsuk Pak [†]

Department of Chemistry, Kyungsung University, Pusan 608-736, Korea
[†]Department of Chemistry, Seoul National University, Seoul 151-740, Korea
Received July 30, 1996

In a recent paper[*Bull. Kor. Chem. Soc.* **17,** 735 (1996)] we reported results of molecular dynamic (MD) simulations for the thermodynamic and structural properties of liquid *n*- alkanes, from *n*- butane to *n*- heptadecane, using three different models. Two of the three classes of models are collapsed atomic models while the third class is an atomistically detailed model. In the present paper we present results of MD simulations for the dynamic properties of liquid *n*- alkanes using the same models. The agreement of two self-diffusion coefficients of liquid *n*- alkanes calculated from the mean square displacements (MSD) *via* the Einstein equation and the velocity auto-correlation (VAC) functions *via* the Green-Kubo relation is excellent. The viscosities of *n*- butane to *n*- nonane calculated from the stress auto-correlation (SAC) functions and the thermal conductivities of *n*- pentane to *n*- decane calculated from the heat-flux auto-correlation (HFAC) functions *via* the Green-Kubo relations are smaller than the experimental values by approximately a factor of 2 and 4, respectively.

Introduction

Green and Kubo[2] showed that the phenomenological coefficients describing many transport processes and time-dependent phenomena in general could be written as integrals over a certain type of function called a time-correlation function. These time-correlation functions play a somewhat similar role in nonequilibrium statistical mechanics that the partition function plays in equilibrium statistical mechanics. The analogy breaks down in one respect. Since the state of thermal equilibrium is unique, a single partition function gives all the thermodynamic properties, but since there are many different kinds of nonequilibrium states, a different time-correlation function for each type of transport process is needed. Determining the appropriate time correlation function to use for a particular transport process of interest is very important.

The Green-Kubo relations (Table 1) are the formal expressions for hydrodynamic field variables and some of the thermodynamic properties in terms of the microscopic variables of an N-particle system. The identification of microscopic expressions for macroscopic variables is made by a process of comparison of the conservation equations of hydrodynamics with the microscopic equations of change for conserved densities. The importance of these relations is three-fold: they provide an obvious method for calculating transport coefficients using computer simulation, a convenient starting point for constructing analytic theories for nonequilibrium processes, and an essential information for designing nonequilibrium molecular dynamics (NEMD) algorithm.

In previous works[3,4] we reported results of equilibrium molecular dynamics (EMD) and NEMD simulations for the thermal transport properties - the self-diffusion coefficients, shear viscosities, and thermal conductivities - of liquid argon[3] at 94.4 K and 1 atm and liquid water[4] at 298.15 K and 1 atm using TIP4P model[5] for the interaction between water molecules. For liquid argon, the overall agreement of the calculated thermal transport properties through EMD and NEMD with the experimental results was quite good.[3] However, in the case of liquid water, the Green-Kubo relations are applied with difficulty to the EMD results since the time-correlation functions are oscillating and not decaying rapidly enough but the NEMD results were found to agree within approximately ±30~40% error bars.[4]

In this paper, we present results of MD simulation studies to investigate the dynamic properties of liquid *n*- alkanes, *n*-butane to *n*- heptadecane, using the above referred models. Further studies also include the investigation of the thermodynamic, structural, and dynamic properties of branched-chain alkanes, and analyses of segmental motions of C-C backbone chains in long chain alkanes.

The paper is organized as follows. Section II contains a brief description of molecular models and MD simulation methods followed by Sec. III which presents the results of our simulations and Sec. IV where our conclusions are summarized.

Table 1. Green-Kubo relations for thermal transport Properties.

$$D_i = \frac{1}{3}\int_0^\infty \langle \mathbf{v}_i(0)\cdot\mathbf{v}_i(t)\rangle dt \quad (1)$$

$$\eta = \frac{V}{kT}\int_0^\infty \langle P_{xy}(0)\cdot P_{xy}(t)\rangle dt \quad (2)$$

$$\lambda = \frac{1}{kT^2}\int_0^\infty \langle J_{Qx}(t)\cdot J_{Qx}(0)\rangle dt \quad (3)$$

where $\mathbf{v}_i$ is the velocity of particle i. P_{xy} is an off-diagonal ($x \neq y$) of the viscous pressure tensor.

$$PV = \sum_{i=1}^{N} m\mathbf{v}_i\mathbf{v}_i + \sum_{i=1}^{N} \mathbf{r}_i\mathbf{F}_i \quad (4)$$

and J_{Qx} is a component of the energy current vector, $\mathbf{J}_Q$:

$$\mathbf{J}_Q V = \sum_{i=1}^{N} E_i\mathbf{v}_i - \frac{1}{2}\sum_i\sum_j \mathbf{r}_{ij}(\mathbf{v}_i\cdot\mathbf{F}_{ij}) \quad (5)$$

Molecular Dynamics Simulations and Molecular Models

In the recent paper,[1] we selected 14 systems for MD simulations using the three different models for liquid *n*- alkanes, from *n*- butane to *n*- heptadecane, all at 293.15 K except for a minor change in temperature to 291.0 K for *n*- butane and to 296.0 K for *n*- heptadecane. Each simulation was carried out in the NVT ensemble: the density and hence the length of cubic simulation box were fixed and listed in Table 1 of Ref. 1. The usual periodic boundary condition in the x-, y-, and z-directions and minimum image convention for pair potential were applied. A spherical cutoff of radius R =2.5 σ, where σ is the Lennard-Jones (LJ) parameter, was employed for all the pair interactions. Gaussian isokinetics[6] was used to keep the temperature of the system constant.

The first model (Model I) is the original Ryckaert and Bellemans' collapsed atomic model[7] in which monomeric units (methylene or methyl) are typically treated as single spheres with masses given in Table 2 of Ref. 1. They interact through an LJ potential between the spheres in different molecules and between the spheres more than three apart on the same molecule. The distance between neighboring spheres is fixed at 1.53 Å and the bond angles are also fixed at 109.47 degrees. In addition to the LJ potential, a C-C-C-C torsional rotational potential is also included which models the missing hydrogen atoms in molecular conformation[7,8] and the potential parameters are also given in Table 2 of Ref. 1. The main benefit of this model is to reduce considerably the amount of computing time by reducing the number of interaction sites. The MD simulations of model I were performed using the Verlet algorithm for the time integration of the equations of motion with a time step of 0.001 ps and the RATTLE algorithm[9] for the bond length and bond angle constraints. MD runs of at least 200,000 time steps each were needed for the liquid alkane system to reach equilibrium. The equilibrium properties were then averaged over 10 blocks of 10,000 time steps (10 ps) for a total of 100,000 time steps (100 ps).

Table 2. Self-diffusion coefficients (D_i, 10^{-9} m^2 s^{-1}) of model II for liquid *n*- alkanes calculated from MSD

n- alkane	D_i	*n*- alkane	D_i	*n*- alkane	D_i
n- butane	7.83	*n*- nonane	2.82	*n*- tetradecane	1.62
	(8.06)[a]	*n*- decane	2.53	*n*- pentadecane	1.55
	[9.49][b]		(2.93)[a]	*n*- hexadecane	1.39
n- pentane	5.91		[3.28][b]	*n*- heptadecane	1.30
n- hexane	4.84	*n*- undecane	2.30		(1.36)[a]
n- heptane	4.02	*n*- duodecane	2.06		[1.43][b]

[a]Model I. [b]Model III.

Model II is the expanded collapsed atomic model which includes a C-C bond stretching potential of harmonic quadratic form and a C-C-C bond angle bending potential of anharmonic cubic form in addition to the LJ and torsional potentials of model I. The equilibrium bond length and bond angle, and the force constants used by Chynoweth *et al.*[10-12] from the work of White and Boville,[13] are given in Table 2 of Ref. 1. For the integration over time of model II, we adopted Gear's fifth-order predictor-corrector algorithm[14] with a time step of 0.0005 ps for all the *n*- alkanes. A total of 100,000 or 150,000 time steps was simulated each for the average and the configurations of molecules were stored every 10 time steps for further analysis.

The last model (model III) is the atomistically detailed model in which the explicit presence of H atoms in the alkane molecule increases the number of interactions in inter and intra LJ potentials between H and H and between C and H atoms, as well as introducing C-H bond stretching, C-C-H and H-C-H bond angle bending, and also terminal C-C-C-H torsional potentials. The bond stretching potential is of the same harmonic quadratic form as model II but the bond angle bending potential has the same harmonic quadratic form rather than that enharmonic cubic of model II. The terminal C-C-C-H torsional potential has a different form to the C-C-C-C of Eq. (1) in Ref. 1. The potential parameters are listed in Table 2 of Ref. 1. The Gear's fifth-order predictor-corrector algorithm[15] was also used with a time step of 0.00033333 ps and the equilibrium properties were averaged for a total of 150,000 time steps (50 ps). We have used a modified LJ parameter for H atom to obtain a reasonable pressure of *n*- butane for model III by comparing the MD calculated pressures for various sets of σ for H atom. The final LJ parameters are listed in Table 2 of Ref. 1.

Results and Discussion

The mean square displacements (MSD) and normalized velocity auto-correlation (VAC) functions of liquid *n*- alkanes are shown in Figures 1 and 2, respectively. As seen in Figures 1 (a), (c), and (e), the further from the center of mass the sites, the larger the MSD's. As the carbon number increases, the slope of MSD is decreased as shown in Figures 1 (b) and (d). The MSD of models I and III for liquid n-butane, *n*- decane, and *n*- heptadecane are shown in Figure 1 (f). The slopes of the MSD of models I and III are larger than those of model II. The self-diffusion coefficients of

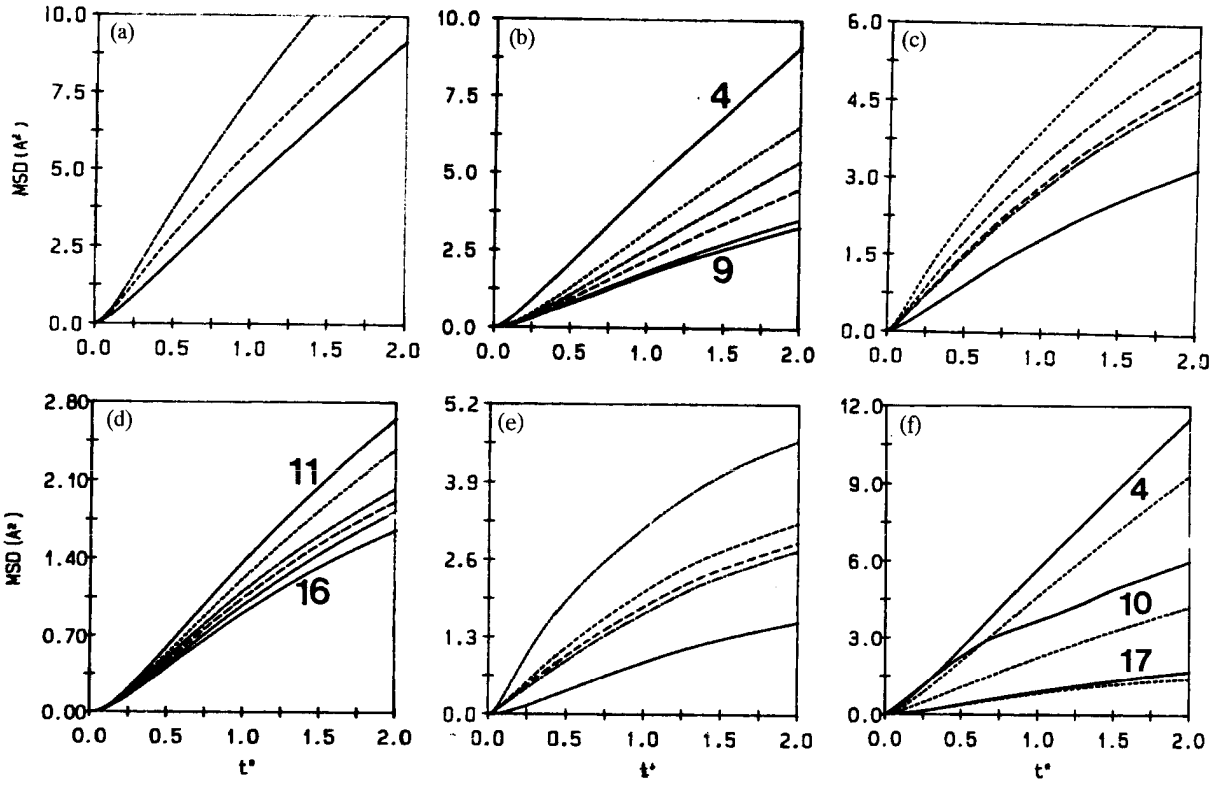

Figure 1. Mean square displacements of model II for liquid *n*- alkanes with t* in ps. (a) center of mass (—), 2nd and 3rd(-----), and 1st and 4th (·····) sites of *n*- butane. (b) center of mass sites of *n*- butane, *n*- pentane, *n*- hexane, *n*- heptane, *n*- octane, and *n*- nonane, where the number represents the carbon number of liquid *n*- alkane. (c) center of mass (—), 4th and 7th (—·—·—), 3rd and 8th (– – –), 2nd and 9th (-----), and 1st and 10th (·····) sites of *n*- decane. (d) center of mass sites of *n*- undecane, *n*- duodecane, and *n*- tridecane, *n*- tetradecane, *n*- pentadecane, and *n*- hexadecane, where he number represents the carbon number of liquid *n*- alkane. (e) center of mass (—), 8th and 10th (—·—·—) 5th and 13th (– – –), 3rd and 15th(-----), and 1st and 17th (·····) sites of sites of *n*- heptadecane, and (f) mean square displacements of models I (·····) and III(—) for liquid *n*- butane(4), *n*- decane(10) and *n*- heptadecane(17).

models I, II, and III for liquid *n*- alkanes calculated from MSD's using the Einstein equation:

$$D_s = \frac{1}{6}\lim_{t\to\infty}\frac{d<|r(t)-r(0)|^2>}{dt} \qquad (6)$$

are listed in Table 2. The calculated self-diffusion coefficient of model I for liquid *n*- butane from our MD simulation is different from that of Edberg *et al.* [15] (8.06/6.14) possibly due to different algorithms used (Verlet and RATTLE in this work[3] and a new procedure to correct for numerical error[16] in Edberg *et al.*). Those of *n*- decane are much different (2.93/5.15) since the MD simulation state points (simulation temperature and density) and simulation algorithms are different, which indicates that the denser and the lower temperature of the system, the lower the self-diffusion coefficient. As the carbon number increases, the self-diffusion coefficient is monotonically decreased.

As seen in Figures 2 (a), (b), (c), and (f), the VAC's of the sites near the center of mass are more oscillating than those near to the ends of the alkyl chains. This seems contrary to the less MSD's of those sites in Figures 1 (a), (c), and (e), but it can be easily understood in terms of the constraint forces on the local segment by the intramolecular interactions - C-C bond stretching and C-C-C bond angle bending. The intramolecular forces exerted on the sites near the center of mass vary much more rapidly than those near to the ends of the alkyl chains and the velocities of the sites have the same trend. Figures 2 (c), (d), and (e) show very little sensitivity of the whole trend of VAC of center of mass to the carbon number. We show the VAC of models I and III for liquid *n*- butane, *n*- decane, and *n*- heptadecane in Figure 2 (g) and (h) respectively. The VAC's of model III are all oscillating functions due to the several intramolecular interactions. In Table 3, the self-diffusion coefficients of models I, II and III for liquid *n*- alkanes calculated from the VAC's using the Green-Kubo relation, Eq. (1), are collected. The self-diffusion coefficient, D_s, can be separated into two parts - kT/m and the integration value of the normalized VAC functions, A

$$A = \int_0^\infty \frac{<v(0)\cdot v(\tau)>}{<v(0)\cdot v(0)>}\,d\tau, \qquad (7)$$

with $D_s = (kT/m)A$ since $m\ v(0)\cdot v(0) = m\ v^2 = 3kT$. The agreement of self-diffusion coefficients, Tables 2 and 3, from the two different routes, Eqs. (6) and (7) is excellent.

The normalized stress auto-correlation (SAC) and heat-flux auto-correlation (HFAC) functions of models I, II and III for liquid *n*- butane, *n*- decane, and *n*- heptadecane are shown in Figures 3 and 4 respectively. The trends are very much similar to each other but the calculated integration value from these normalized auto-correlation

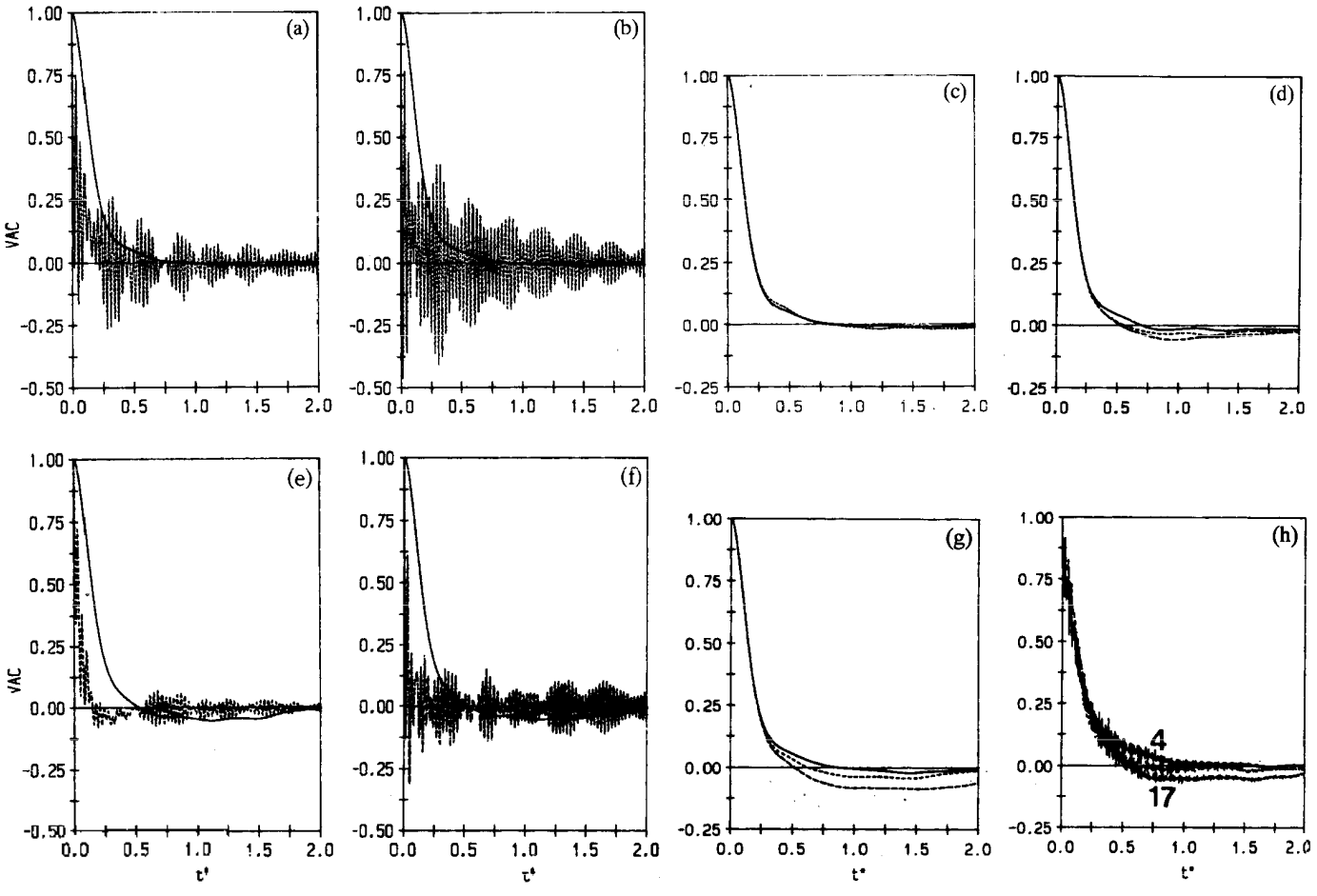

Figure 2. Normalized velocity auto-correlation functions of model II for liquid *n*- alkanes with t* in ps. (a) center of mass (—), and 1st and 4th(-----) sites of n-butane. (b) center of mass (—), and 2nd and 3rd(-----) sites of *n*- butane. (c) center of mass sites of *n*- butane (—), *n*- pentane(-----), and *n*- hexane (·····). (d) center of mass sites of *n*- heptane (—), *n*- octane(-----), and *n*- nonane (·····). e) center of mass (—), 1st and 10th(-----) sites of *n*- decane. (f) center of mass (—) 3rd and 8th(-----) sites of *n*- decane. (g) normalized velocity auto-correlation functions of model I for liquid *n*- butane (—), *n*- decane (·····) and *n*- heptadecane(-----), and (h) of model III for liquid *n*- butane, *n*- decane and *n*- heptadecane, where the number represents the carbon number of liquid *n*- alkane.

Table 3. Self-diffusion coefficients(D, 10^{-9} m^2 s) of model II for liquid *n*- alkanes calculated from VAC. The value of A(ps) is the integration value of Eq.(7) and kT m in 10^{-21} m^2 s^{-2}.

n- alkane	kT m	A	D	*n*- alkane	kT m	A	D
n- butane	42.32	0.1719	7.28	*n*- undecane	14.93	0.1483	2.21
	(41.30	0.1782	7.36)[a]	*n*- duodecane	13.67	0.1441	1.97
	|44.39	0.2075	9.21|[a]	*n*- tridecane	12.60	0.1291	1.63
n- pentane	33.58	0.1732	5.82	*n*- tetradecane	11.70	0.1306	1.53
n- hexane	27.85	0.1719	4.79	*n*- pentadecane	10.91	0.1339	1.46
n- heptane	23.79	0.1660	3.95	*n*- hexadecane	10.22	0.1313	1.34
n- octane	20.62	0.1424	2.94	*n*- heptadecane	9.614	0.1318	1.27
n- nonane	18.29	0.1386	2.53		(9.336	0.1388	1.30)[b]
n- decane	16.44	0.1383	2.27		|9.406	0.1467	1.38|
	(15.81	0.1505	2.38)[b]				
	|17.15	0.1565	2.68|[b]				

[a]Model I. [b]Model III and in the calculation of D_z the mass of C atoms only is considered.

functions are very different. The viscosities and thermal conductivities of models I, II, and III for *n*- alkanes calculated from the Green-Kubo relations, Eqs. (2) and (3) are listed in Tables 4 and 5. The viscosity, η, and thermal conductivity, λ, are also separated into two parts respectively - $V \cdot P_{xy}$ - $^2/kT$ and the integration value of the normalized SAC functions, B:

$$B = \int_0^\infty \frac{\langle P_{xy}(0) \cdot P_{xy}(\tau) \rangle}{\langle P_{xy}(0) \cdot P_{xy}(0) \rangle} d\tau \quad (8)$$

and $V \cdot J_{Qx} \cdot {}^2/kT^2$ and the integration value of the normalized HFAC functions, C:

$$C = \int_0^\infty \frac{\langle J_{Qx}(0) \cdot J_{Qx}(\tau) \rangle}{\langle J_{Qx}(0) \cdot J_{Qx}(0) \rangle} d\tau \quad (9)$$

with $\eta = \frac{V \cdot P_{xy}{}^2}{kT} B$ and $\lambda = \frac{V \cdot J_{Qx}{}^2}{kT^2} C$.

The experimental viscosity of *n*- butane at density 0.583 g/cc and temperature 291 K is 0.19 cP.[17] Those of *n*- pentane, *n*- hexane, *n*- heptane, *n*- octane, and *n*- nonane at 298 K are 0.240, 0.326, 0.409, 0.542, and 0.711 cP,[18] respectively. Our results for *n*- butane to *n*- nonane are smaller than the experimental values by approximately a factor of 2. An equilibrium molecular dynamics (EMD) simulation study for n-butane at the same state arrived at 0.26 cP[19] *via* the Green-Kubo relation. Several non-equilibrium molecular dynamics (NEMD) simulation studies reported different values – 0.24[20] and 0.175[21] for model I, and 0.168[22] and 0.171[21] for model II. The experimental viscosity of *n*- decane at 0.6136 g/cc and 480 K is 0.196 ± 0.006 cP.[17] An NEMD simulation study predicted an accurate result for the viscosity of *n*- decane at the same state – 0.190 ± 0.015 cP.[20] Another EMD and NEMD simulation studies reported better results – 0.191 ± 0.012 and 0.197 ± 0.003,[24] respectively. Unfortunately no experimental values at 0.730 g/cc and 293, 15 K are available to compare with our results for *n*- decane. As the carbon number increases, the calculated viscosity is generally increased as shown in Table 4.

The experimental thermal conductivities of *n*- pentane, *n*- hexane, *n*- heptane, *n*- octane, *n*- nonane, and *n*- decane at 298 K are 0.1348, 0.1375, 0.1403, 0.1451, 0.1412, and 0.140118, respectively. It seems that the thermal conductivity of liquid *n*- alkane is independent of the carbon number of *n*- alkane. Our results for *n*- pentane to *n*- decane are smaller than the experimental values by approximately a factor of 4. The disagreement of our MD simulation results for the viscosities and thermal conductivities of liquid *n* -alkanes with the experimental values may be possibly involved in several aspects, but the most significant point is due to the limitation of equilibrium MD simulation using

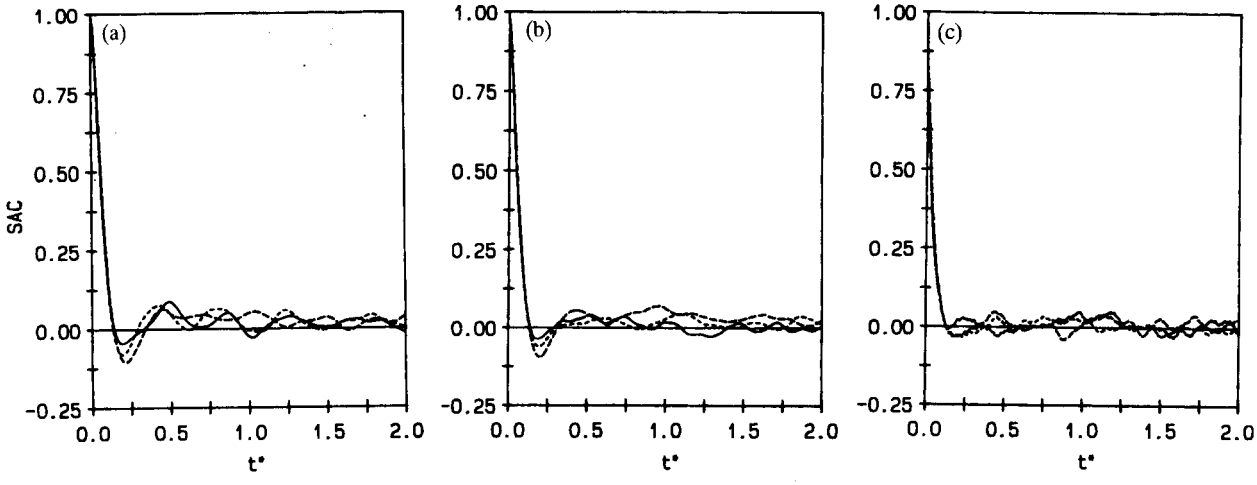

Figure 3. Normalized stress auto-correlation functions of models (a) I (b) II and (c) III for liquid *n*- butane (—), *n*- decane(-----), and *n*-heptadecane (·····) with t* in ps.

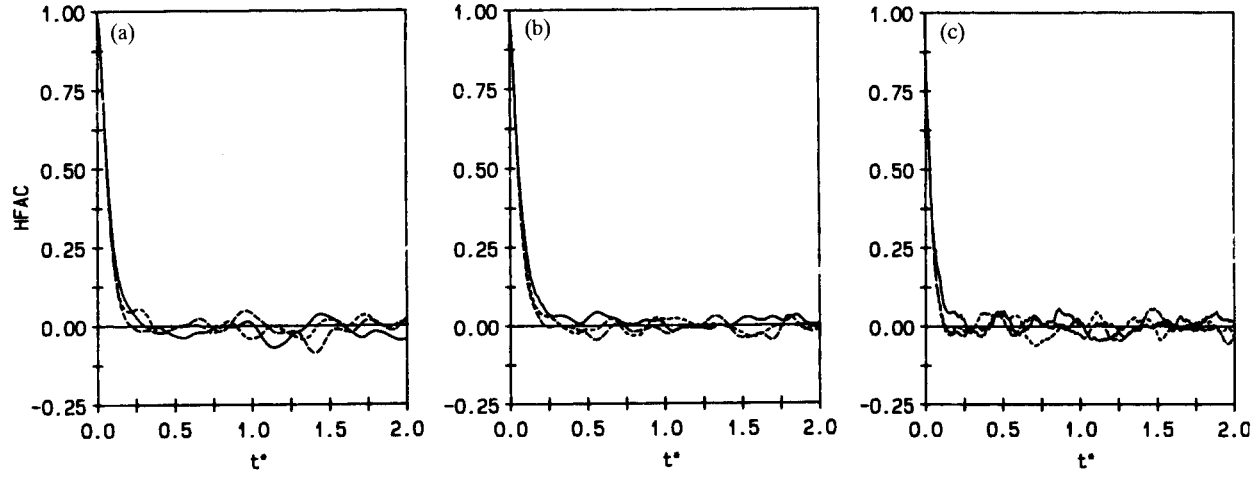

Figure 4. Normalized heat-flux auto-correlation functions of models (a) I, (b) II, and (c) III for liquid *n*- butane (—), *n*- decane(-----), and *n*- heptadecane (·····) with t* in ps.

Table 4. Viscosities (η, cP) of model II for liquid *n*- alkanes calculated from SAC. The value of B(ps) is the integration value of Eq.(8) and $V/P_{xy}^2 \cdot kT$ is cP ps.

n- alkane	$V/P_{xy}^2/kT$	B	η	*n*- alkane	$V/P_{xy}^2/kT$	B	η
n- butane	1.686	0.06448	0.109	*n*- undecane	5.265	0.06095	0.321
	(1.486	0.07983	0.119)[a]	*n*- duodecane	5.630	0.05895	0.332
	[2.425	0.04452	0.108][b]	*n*- tridecane	6.331	0.06518	0.413
n- pentane	2.143	0.05908	0.127	*n*- tetradecane	6.371	0.06544	0.417
n- hexane	2.651	0.05948	0.158	*n*- pentadecane	7.373	0.06903	0.509
n- heptane	3.074	0.05775	0.178	*n*- hexadecane	7.325	0.06534	0.479
n- octane	3.750	0.07613	0.286	*n*- heptadecane	7.615	0.06659	0.507
n- nonane	4.201	0.06668	0.280		(6.722	0.07978	0.536)[a]
n- decane	4.852	0.06442	0.313		[12.18	0.04427	0.539][b]
	(4.230	0.07983	0.342)[a]				
	[7.275	0.03956	0.288][b]				

[a]Model I. [b]Model III and in the calculation of η, the mass of C atoms only is considered.

Table 5. Thermal conductivities (λ, J/s · m · K) for liquid *n*- alkanes calculated from HFAC. The value of C(ps) is the integration value of Eq. (9) and $V/J_{xx}^2 \cdot kT^2$ in J/s · m · K · ps.

n- alkane	$V/J_x^2 \cdot kT^2$	C	λ	*n*- alkane	$V/J_x^2 \cdot kT^2$	C	λ
n- butane	0.6079	0.09459	0.0575	*n*- undecane	0.5662	0.06724	0.0363
	(0.5248	0.07035	0.0369)[a]	*n*- duodecane	0.5045	0.06418	0.0270
	[0.7783	0.04836	0.0376][b]	*n*- tridecane	0.5006	0.05348	0.0282
n- pentane	0.5445	0.07530	0.0410	*n*- tetradecane	0.4816	0.05634	0.0279
n- hexane	0.5767	0.07959	0.0459	*n*- pentadecane	0.5055	0.05799	0.0317
n- heptane	0.5469	0.09527	0.0521	*n*- hexadecane	0.4874	0.06269	0.0349
n- octane	0.5618	0.08777	0.0493	*n*- heptadecane	0.5347	0.07155	0.0345
n- nonane	0.5197	0.06511	0.0338		(0.4556	0.06716	0.0306)[a]
n- decane	0.5297	0.06724	0.0356		[0.7431	0.03374	0.0251][b]
	(0.4532	0.07190	0.0326)[a]				
	[0.7396	0.03808	0.0282]				

[a]Model I. [b]Model III and in the calculation of λ, the mass of C atoms only is considered.

Green-Kubo relations for the thermal transport properties of liquid *n*- alkanes, and that explains why the non-equilibrium MD simulation has been developed recently.

Concluding Remarks

We have carried out a series of MD simulations of liquid *n*- alkanes, from *n*- butane to *n*- heptadecane, using three different models. Two of the three classes of models are collapsed atomic models while the third class is an atomistically detailed model. In a recent paper,[1] we reported the MD simulation results for the thermodynamic and structural properties of liquid *n*- alkanes. Excellent agreement of the results of model I for *n*- butane from different MD algorithms, ours and those of Edberg *et al.*,[16] confirmed the validity of our whole set of MD simulations of model II for 14 liquid *n*- alkanes and of models I and III for liquid *n*- butane, *n*- decane, and *n*- heptadecane. The thermodynamic and structural properties of model I and II were very similar to each other and the thermodynamic properties of model III for the three *n*- alkanes are not much different from those of models I and II. However, the structural properties of model III were very different from those of model I and II as seen from the radial distribution functions, the average end-to-end distances, and the root-mean-squared radii of gyration.

In the present paper we report results of MD simulations for the dynamic properties of liquid *n*- alkanes using the same models. The velocity auto-correlation (VAC) functions of the sites near the center of mass are more oscillating than those near to the ends of the alkyl chains and this seems contrary to the less mean square displacements (MSD) of those sites, but it can be easily understood in terms of the constraint forces on the local segment by the intramolecular interactions. The agreement of two self-diffusion coefficients of liquid *n*- alkanes calculated from the MSD's *via* the Einstein equation and the VAC functions *via* the Green-Kubo relation is excellent. The trends of the normalized stress auto-correlation (SAC) and heat-flux auto-correlation (HFAC) functions of models I, II and III for liquid *n*- butane, *n*- decane and *n*- heptadeane are very much similar to each other but the calculated integration value from these normalized auto-correlation functions are very different. The viscosities of *n*- butane to *n*- nonane calculated from the SAC functions and the thermal conductivities of *n*- pentane to *n*- decane calculated from the HFAC functions *via* the Green-Kubo relations are smaller than the experimental values by approximately a factor of 2 and 4, respectively.

Acknowledgment. This work was supported by Basic Science Research Institute Program, Ministry of Education (BSRI-95-3414). S. H. L. thanks the Korea Institute of Sci-

ences and Technology for access to the Cray-C90 super computer.

References

1. Lee, S. H.; Lee, H.; Pak, H.; Rasaiah, J. C. *Bull. Kor. Chem. Soc.* **1996,** *17,* 735.
2. (a) Green, M. S. *J. Chem. Phys.* **1951,** *19,* 249. (b) *ibid.* **1952,** *20,* 1281. (c) *ibid.* **1954,** *22,* 398. (d) Kubo, R. *J. Phys. Soc. Japan* **1957,** *12,* 570.
3. Moon, C. B.; Moon, G. K.; Lee, S. H. *Bull. Kor. Chem. Soc.* **1991,** *12,* 309.
4. Lee, S. H.; Moon, G. K.; Choi, S. G. *Bull. Kor. Chem. Soc.* **1991,** *12,* 315.
5. (a) Jorgensen, W. L.; Chandrasekhar, J.; Madura, J. D.; Impey, R. W.; Klein M. L. *J. Chem. Phys.* **1983,** *79,* 926. (b) Jorgensen W. L.; Madura J. D. *Mol. Phys.* **1985,** *56,* 1381.
6. Evans D. J.; Hoover W. G.; Failor B. H.; Moran B.; Ladd A. J. C. *Phys. Rev. A.* **1983,** *28,* 1016. Simmons A. D.; Cummings P. T. *Chem. Phys. Lett.* **1986,** *129,* 92.
7. Ryckaert J. P.; Bellemans A. *Discuss. Faraday Soc.* **1978,** *66,* 95.
8. Wielopolsky P. A.; Smith E. R. *J. Chem. Phys.* **1986,** *84,* 6940.
9. Allen M. P.; Tildesley D. J. *Computer Simulation of Liquids;* Oxford, Oxford Univ. Press.; 1987.
10. Andersen H. C. *J. Chem. Phys.* **1983,** *52,* 24.
11. Chynoweth S.; Klomp U. C.; Scales L. E. *Comput. Phys. Commun.* **1991,** *62,* 297.
12. Chynoweth S.; Klomp U. C.; Michopoulos Y. *J. Chem. Phys.* **1991,** *95,* 3024.
13. Berker A.; Chynoweth S.; Klomp U. C.; Michopoulos Y. *J. Chem. Soc., Faraday Trans.* **1992,** *88,* 1719.
14. White D. N. J.; Boville M. J. *J. Chem. Soc. Perkin Trans.* **1977,** *2,* 1610.
15. Gear C. W. *Numerical Initial Value Problems in Ordinary Differential Equation;* Englewood Cliffs NJ, Prentice-Hall; 1971.
16. Edberg R.; Evans D. J.; Morriss G. P. *J. Chem. Phys.* **1986,** *84,* 6933.
17. Stephan K.; Lucas K. *Viscosity of Dense Fluids;* Plenum: New York: 1979.
18. Weast R. C.; Astle M. J. *CRC Handbook of Chemistry and Physics,* 63rd ed.; CRC press: Boca Ranton, 1982-1983.
19. Marechal G.; Ryckaert J. P. *Chem. Phys. Lett.* **1983,** *101,* 548.
20. Edberg R.; Morriss G. P.; Evans D. J. *J. Chem. Phys.* **1987,** *86,* 4555.
21. Lee S. H.; Cummings P. T. *Mol. Sim.* **1996,** *16,* 229.
22. Chynoweth S.; Klomp U. C.; Michopoulos Y. *J. Chem. Phys.* **1991,** *95,* 3024.
23. Mundy C. J.; Siepman J. I.; Klein M. L. *J. Chem. Phys.* **1995,** *102,* 3376.
24. Cui S. T.; Cummings P. T.; Cochran H. D. *J. Chem. Phys.* **1996,** *104,* 255.

The Reaction of 6,7-Dichloro-5,8-quinoxalinedione with Aromatic and Aliphatic Dinucleophiles and Molecular Modeling Study of Their Intercalation Complexes

Hee-Won Yoo [†], Myung-Eun Suh [‡], Kye Jung Shin, and Sang-Woo Park*

[†]Division of Medicinal Chemistry, College of Pharmacy, Ewha Womans University, Seoul 120-750, Korea
[‡]Division of Applied Science, Korea Institute of Science and Technology, Seoul 120-750, Korea
Received November 7, 1996

The angular and planar heterocyclic compounds containing nitrogen, sulfur and oxygen were synthesized by reaction of 6,7-dichloro-5,8-quinoxalinedione with aromatic and aliphatic dinucleophiles. Nucleophilic reactivity was somewhat different between 2,3-dichloro-1,4-naphthoquinone and 6,7-dichloro-5,8-quinolinedione with dinucleophiles. The distribution of electron in heterocycle appeared to contribute to this difference. The intercalation comple of planar heterocyclic compound between GC/GC base pairs showed the optimum intercalation but the intercalation of angular heterocyclic compound was not good. Thus, the planar compound was expected to have antitumor activity.

Introduction

The reaction of 2,3-dichloro-1,4-naphthoquinone and 6,7-dichloro-5,8-quinolinedione with nucleophiles was investigated for a long time. However, the reaction of the analogue 6,7-dichloro-5,8-quinoxalinedione (**1**) with nucleophiles was rarely reported because the total yield of **1** was only 1.1%.[1] The new method, in which the total yield was 27%, was developed recently.[2] Dichloro compound showed the diverse reactivity with nucleophiles and produced various heterocyclic compounds.[3] We synthesized heterocycles by reaction of **1** with aromatic and aliphatic dinu-